DOI: 10.6060/ivkkt.20246709.7108

УДК: 544.424.4+661.634.2

СИНТЕЗ АЛЮМОФОСФАТНОЙ СВЯЗКИ: ВЛИЯНИЕ РЕАКЦИОННОЙ СПОСОБНОСТИ ГИДРОКСИДА АЛЮМИНИЯ

Н.В. Филатова, Н.Ф. Косенко, А.С. Артюшин, К.С. Садкова

Наталья Владимировна Филатова (ORCID 0000-0001-7552-3496)*, Надежда Федоровна Косенко (ORCID 0000-0001-8806-7530), Артем Сергеевич Артюшин, Ксения Сергеевна Садкова

Кафедра технологии керамики и электрохимических производств, Ивановский государственный химико-технологический университет, пр. Шереметевский, 7, Иваново, Российская Федерация, 153000
E-mail: zyanata@mail.ru*, nfkosenko@gmail.com, xavier.guerra@mail.ru, sadkovaks@mail.ru

Широкое промышленное применение растворов кислого фосфата алюминия как связующих для изготовления огнеупоров и других композиционных материалов зачастую ограничено их низкой стабильностью при хранении, особенно при молярном отношении P_2O_5 /Al_2O_3 (P/Al) менее 3,0. Важнейшим фактором устойчивости фосфатных связок является степень их однородности, достигаемой в процессе синтеза. Внимание к степени прозрачности связок обусловлено тем, что взвешенные частицы твердой фазы, не полностью растворившиеся в фосфорной кислоте, представляют собой зародыши для последующей спонтанной поликонденсации, а, следовательно, к нерегулируемому затвердеванию дисперсии при хранении. Нежелательным результатом такого процесса является значительное сокращение срока живучести связок. С помощью нефелометрического анализа показано, что при фиксированной длительности синтеза максимальную однородность имели связки, полученные при растворении гидроксида алюминия в виде гиббсита $Al(OH)_3$ после обработки при 200-250 °С (Г200, Г250) и гидроксида алюминия в форме байерита в ортофосфорной кислоте (ОФК). Методом ИК-спектрального анализа показано, что составы жидкой фазы и осадка, выделенных из алюмофосфатной связки, различались независимо от температуры термообработки гиббсита, а значит, фильтрация способна нарушить заданное молярное соотношение P/Al. Следовательно, в ходе синтеза связки целесообразно добиваться максимально полного растворения вещества, вводящего Al_2O_3, в том числе и за счет повышения реакционной способности последнего. Сравнительно быстрое растворение гиббсита, термообработанного при 200 и 250 °С (Г200, Г250), а также байерита в ортофосфорной кислоте могло свидетельствовать об их повышенной химической активности.

Ключевые слова: фосфатные связующие, алюмофосфатная связка, дигидрофосфат алюминия, реакционная способность гидроксида алюминия, гиббсит, байерит, бёмит, однородность связки, отношение P/Al

AN ALUMINUM-PHOSPHATE BINDER SYNTHESIS: THE EFFECT OF THE ALUMINUM HYDROXIDE REACTIVITY

N.V. Filatova, N.F. Kosenko, A.S. Artyushin, K.S. Sadkova

Natalya V. Filatova (ORCID 0000-0001-7552-3496)*, Nadezhda F. Kosenko (ORCID 0000-0001-8806-7530), Artyom S. Artyushin, Ksenia S. Sadkova

Department of Ceramics Technology and Electrochemical Production, Ivanovo State University of Chemistry and Technology, Sheremetevskiy ave., 7, Ivanovo, 153000, Russia
E-mail: zyanata@mail.ru*, nfkosenko@gmail.com, xavier.guerra@mail.ru, sadkovaks@mail.ru

The wide industrial use of acid aluminum phosphate solutions as binders for refractories and other composites is often limited by their low storage stability, especially at the molar ratio P_2O_5 / /Al_2O_3 (P/Al) < 3.0. The most important factor in the phosphate binder's stability is the degree of their homogeneity achieved in the process of synthesis. The attention to the degree of binder's

transparency is because suspended particles are nuclei for subsequent spontaneous polycondensation, and therefore too unregulated solidification of a dispersion during storage. An undesirable result of this is a significant reduction in the binder's survivability. The nephelometry showed that at a fixed synthesis duration, the binders obtained by dissolving gibbsite after treatment at 200-250 °C (G200, G250) and bayerite in orthophosphoric acid (OPA) had the maximum homogeneity. IR spectra showed that the compositions of the liquid phase and the precipitate differed regardless of the gibbsite heat treatment temperature, which means that filtration is able to violate the specified P/Al ratio. Therefore, during synthesis, it is advisable to achieve the most complete dissolution of the substance introducing Al_2O_3, including by increasing the reactivity of the latter. The relatively rapid dissolution of G200, G250 and bayerite in the OPA solutions could indicate their increased chemical activity.

Key words: phosphate binders, aluminum phosphate binder, aluminum dihydrogen phosphate, aluminum hydroxide reactivity, gibbsite, bayerite, boehmite, binder homogeneity, P/Al ratio

Для цитирования:
Филатова Н.В., Косенко Н.Ф., Артюшин А.С., Садкова К.С. Синтез алюмофосфатной связки: влияние реакционной способности гидроксида алюминия. *Изв. вузов. Химия и хим. технология*. 2024. Т. 67. Вып. 9. С. 126–133. DOI: 10.6060/ivkkt.20246709.7108.

For citation:
Filatova N.V., Kosenko N.F., Artyushin A.S., Sadkova K.S. An aluminum-phosphate binder synthesis: the effect of the aluminum hydroxide reactivity. *ChemChemTech [Izv. Vyssh. Uchebn. Zaved. Khim. Khim. Tekhnol.]*. 2024. V. 67. N 9. P. 126–133. DOI: 10.6060/ivkkt.20246709.7108.

INTRODUCTION

For eight decades, inorganic phosphates have been known as chemical binders with increasing practical applications due to their resistance to high temperatures, low-temperature curing, low production costs and ease of preparation [1], excellent adhesive strength [2], and increased resistance to chemical corrosion [3] and oxidation [4]. Phosphate binders are of particular interest in the field of refractories due to their good adhesion and reduced risk of cracking at high heating rates after hardening [5, 6]. Phosphate-based refractories have great potential for use in the petrochemical industry, as they have the necessary properties in the temperature range used in catalytic cracking [7]. Phosphate bonded refractories can be used as repair materials due to their short setting time and good thermomechanical properties [5]. Oxide-phosphates have good resistance to low temperatures [8].

Currently, there are many commercially available phosphate compounds based on aluminum (more than 50) [5]. They are used as flame retardant additives in adhesives, antifreezes, paints. Aluminum phosphates are mainly used, which provide good strength, stability at high temperatures, and abrasion resistance [9], low shrinkage during hardening, low cost and short production cycle [10]. Alumina phosphate binders (APBs) have good application prospects in fields such as aerospace, coatings, composites due to their high adhesion strength, dielectric properties, structure design capabilities, and sintering temperature reduction. For example, composites with an alumina phosphate (AP) matrix reinforced with quartz fiber are expected to become materials for the next generation of hypersonic fairings. AP coating provides excellent radiation cooling [11].

Among APBs, aluminum dihydrogen phosphate $Al(H_2PO_4)_3$ (ADHP), also called monoaluminium phosphate (MAP), stands out, which is recognized as one of the most effective binders due to its good mechanical and adhesive strength, high solubility in water, abrasive and corrosion resistance, ability to react with basic and amphoteric raw materials at low temperatures [5]. This non-toxic and environmentally friendly cementitious substance is widely used in high-temperature adhesives, ceramics, refractories, composite materials, and anti-corrosion coatings [12]. Chemically bonded alumina phosphate ceramics offer various benefits, including good corrosion resistance and strength at high temperatures. Composites based on ADHP and mullite with excellent mechanical and thermal properties are promising for high-strength thermal insulation in chemical, metallurgical, pharmaceutical, aerospace, and other fields [12]. APBs also play an important role in such areas as the fairings manufacture, flame retardants, porous materials, inorganic membranes, etc. [11]. Ceramics were obtained from porous silicon carbide (SiC) [13] and SiO_2 [14] with ADHP. 3D printing of Al_2O_3 ceramic structures with ultra-low shrinkage is realized through the introduction of

ADHP as a ceramic precursor [15]. The potential use of APBs in the processing of strontium-containing waste has been noted [16]. The flammability and spread of fire in a mixed geopolymer of fly ash and metakaolin with the addition of ADHP and aluminum phosphate $AlPO_4$ have been evaluated [17]. ADHP is used for phosphate ceramic coatings on stainless steel [4, 18]. A porous foam made of carbon fiber with an aluminum phosphate has been proposed [19]. The possibility of improving the lubricity and wear resistance of graphite coating at elevated temperatures due to a phosphate binder has been noted [20]. A heat-resistant adhesive was obtained for the repair and bonding of titanium alloys [21]. A practical adhesive made of aluminum phosphates as a matrix and SiO_2/B_4C has been developed [1]. APBs are suitable for the manufacture of wood-based panels, as they can replace formaldehyde-based adhesives in the woodworking industry [22]. APs have been used to restore destroyed Terracotta warriors and horses at the Xianyang Museum, fractured sandstone in the Yungang Grottoes in Datong, and the Thousand Buddha Cliff in China. In [24], the potential of acidic solutions of aluminum phosphate to improve the characteristics of kaolin phosphate geopolymer binders obtained at room temperature was evaluated.

The thermal evolution of aluminum phosphates has been repeatedly considered in the scientific literature [17, 25-29]. These compounds exhibit several phase transitions when heated, which are mainly characterized by polymerization and condensation reactions to form tripoly- and metaphosphates. The heating to a temperature above 1200 °C causes the metaphosphates transition to $AlPO_4$ with the simultaneous release of phosphorus oxide P_2O_5. The reaction patterns of aluminum phosphates are highly dependent on the molar ratio of P_2O_5/Al_2O_3 (P/Al), heat treatment, reaction atmosphere, etc. [3].

There are many factors to consider when selecting the P/Al ratio for the synthesis and study of APBs. For example, the lowest curing temperature was observed at P/Al ratio of 2.49 [2]. At P/Al = 3:1, the only reaction product was $Al(H_2PO_4)_3$ [24, 25, 27, 28] with the best adhesion strength. With an increase in the concentration of phosphoric acid solution in the range of 60–80%, the viscosity increased due to a greater degree of polymerization of phosphorus-oxygen tetrahedra [27]. Industrial use of acid aluminum phosphate solutions is often limited by their low storage stability, especially at P/Al < 3.0. A white sediment fell after a few days/weeks of APB storage with P/Al from 2 to 3. A solution with P/Al ≥ 3 is stable for a long time [9, 11, 29]. The destabilization mechanism included polymerization with the formation of insoluble aluminum phosphate compounds, and a decrease in the solution concentration could improve its stability. Boron supplementation increased stability by reducing the number of active sites on the aluminum phosphate forms available for polymerization and by increasing the viscosity of the solution, which restricted the movement of aluminum phosphate forms [11]. At the same time, it should be borne in mind that the adhesion characteristics and heat resistance increased with a decrease in the P/Al ratio [10]. With a P/Al increase in the initial solution, the polymerization rate increased, so $Al(PO_3)_3$[A] was formed at lower temperatures (already at 350 °C after heating the solution with a P/Al ratio of 3.5) [9]. If the P/Al ratio was greater than 3, then a solution contained residual phosphoric acids after heat treatment [29], which could be critical for some industrial applications (corrosion of furnaces with volatile P_2O_5) [26]. The compressive strength of the samples increased with an increase in P/Al due to the formation of Al-O-P bonds during dehydration when the temperature increased [28]. The main advantages (+) and disadvantages (-) of low and high P/Al values in APBs are summarized in Table.

Table

Influence of the P/Al ratio on the most important APBs characteristics

***Таблица.* Влияние отношения P/Al на важнейшие характеристики алюмофосфатного связующего (АФС)**

P/Al < 3	P/Al > 3
(-) Low stability (+) Higher curing speed (+) Lower hygroscopicity (+) Fewer microcracks in the hardened binder (+) Better adhesion (+) Higher heat resistance	(+) Higher stability (+) Strength increases (-) Hardening time increases (-) Presence of residual phosphoric acids

Aluminum hydroxide [9, 12, 28, 30] or Al_2O_3 [9] was most often used as a source of alumina. Aluminum nitrate and chloride [30] and pseudo boehmite [31] were also tested. Orthophosphoric acid was usually diluted to 60-65% for synthesis, a 48% solution was only used to obtain self-flowing concretes [17].

In this paper, an attempt is made to compare the use of different forms of $Al(OH)_3$: bayerite and gibbsite, which have different reactivity, in the synthesis of APBs with a P/Al ratio of 3.0, as well as the behavior of prepared binders.

MATERIALS AND EXPERIMENTS

The following reagents were used: 85% orthophosphoric acid (OPA) H_3PO_4, JSC "Khimreaktiv",

"pure", GOST 6552-80; aluminum hydroxide $Al(OH)_3$ (gibbsite), JSC "Khimreaktiv", "pure for analysis", GOST 11841-76, bayerite $Al(OH)_3$, the synthesis and characteristics of which were described earlier [32]. Bayerite was used for the synthesis of APB without additional processing, and gibbsite was subjected to heat treatment at 50, 100, 150, 200, 250, 300, 350, 400, 450, 500 and 550 °C. Heat-treated samples were designated G50, G100, G150, G200, G250, G300, G350, G400, G450, G500 and G550, respectively.

Thermal analysis (TG/DSC) was performed using a NETZSCH STA 449F5 Jupiter: heating rate of 5 °C/min in a flowing air atmosphere (50 ml/min) with α-Al_2O_3 as the standard substance. IR spectra were obtained on the Avatar 360-FT-IR spectrometer (Nicolet). X-ray phase analysis was carried out at the DRON-6 facility with a copper anode (λ = 1.54 Å, 40 kV, 100 mA). The turbidity of the binders was assessed using a nephelometer 2100 AN (HACH). Specific electrical conductivity was measured at 20 °C on a laboratory conductometer ANION 4120.

To prepare APBs, the acid was diluted with distilled water up to 65 %, heated in a water bath to 85 °C, and then, continuing heating and continuous mixing, Al hydroxide was added in portions in an amount that provided a molar ratio of P/Al 3.0. The synthesis duration was 1 h. Naturally cooled binders were stored in well-closed vessels. The density of binders was within 1.46–1.51 g/cm^3; specific electrical conductivity 3.1–4.5 mS·cm^{-1}; pH 0.97–1.02 (20 °C); viscosity 0.74–0.82 Pa·s (20 °C).

RESULTS

Aluminum oxide-hydroxide compounds have different reactivity, ranging from extremely low in corundum α-Al_2O_3 to high in alumogel and bayerite. We compared the results of APB synthesis using a freshly precipitated and dried bayerite and gibbsite, which was subjected to heat pretreatment in the temperature range of 50-550 °C.

By dissolving bayerite in OPA according to the above method, a viscous transparent liquid was obtained, while the use of heat-treated gibbsite gave ambiguous results. Under the same synthesis conditions, the original gibbsite and G50 formed turbid binders; G100 and G150 formed weakly turbid solutions, G200 and G250 – transparent solutions; for G300–G550, a more pronounced sediment release was observed. To quantify the degree of turbidity, nephelometric measurements were carried out (Fig. 1). Attention to the binder transparency is due to the fact that suspended particles are nuclei for subsequent spontaneous polycondensation, and therefore to the unregulated dispersion solidification during storage. An undesirable result of this is a significant reduction in the binder's survivability, which sometimes makes it impossible to use them in practice.

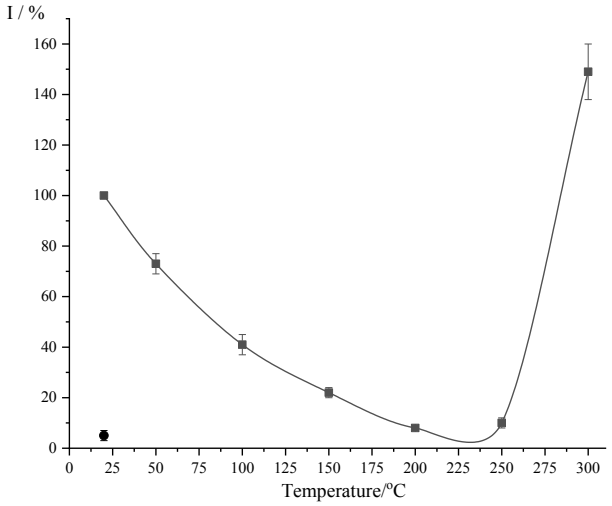

Fig. 1. Relative nephelometer signal intensity for APBs obtained under comparable conditions using gibbsite processed at different temperatures. In the lower left corner is a dot for bayerite-based APB

Рис. 1. Относительная интенсивность сигнала нефелометра для АФС, полученных в сопоставимых условиях с использованием гиббсита, обработанного при разных температурах. В левом нижнем углу точка для АФС на основе байерита

The rapid solubility of bayerite in OPA can apparently be explained by the high reactivity of the freshly precipitated reagent.

For all synthesized binders, identical diffractograms were obtained, one of which is presented in Fig. 2. It shows that the binders with a molar ratio of P/Al = 3.0 are monophasic aluminum dihydrogen phosphate.

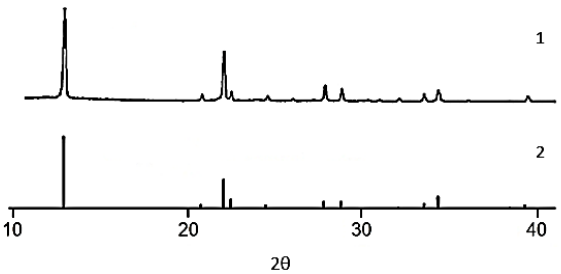

Fig. 2. Diffractogram of APB obtained from gibbsite (1); a bar diagram of the ADHP standard $Al(H_2PO_4)_3$ [27] is given (2)

Рис. 2. Дифрактограмма АФС, полученной из гиббсита (1); приведена штрих-диаграмма эталона ДГФА $Al(H_2PO_4)_3$ (2) [27]

TG and DSC curves for gibbsite-based APB (Fig. 3) indicate stepwise transformations of aluminum dihydrogen phosphate.

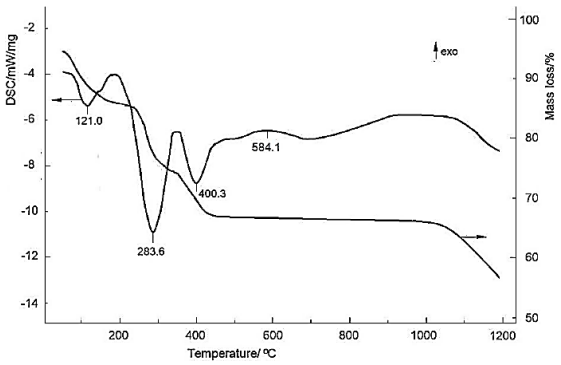

Fig. 3. TG/DSC curves of gibbsite-derived APB
Рис. 3. ТГ/ДСК кривые АФС, полученной из гиббсита

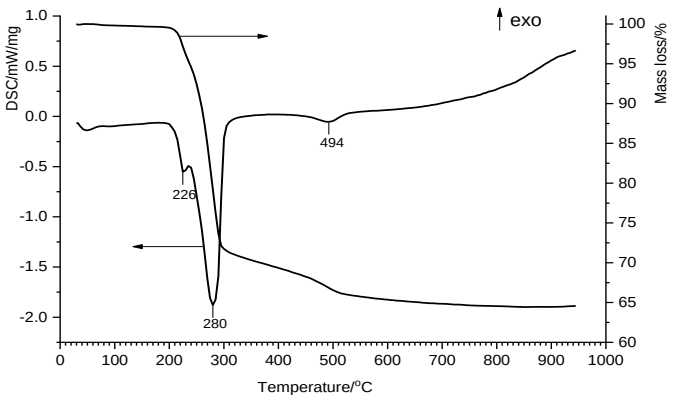

Fig. 4. TG/DSC curves for gibbsite
Рис. 4. ТГ/ДСК кривые для гиббсита

The initial weight loss (up to 195-200 °C) can be attributed to the smooth removal from the binder of adsorption water, which was present in some amount despite the preliminary drying of the substance, due to its strong hygroscopicity. With a further increase in temperature (up to ~345 °C), a sharp drop in weight was observed (by 11.7% on dry matter) with a significant endothermic effect at 283.6 °C. This corresponded to the dehydration of dihydrogen phosphate $Al(H_2PO_4)_3$ to tripolyphosphate $AlH_2P_3O_{10}$. The next stage of dehydration (6.9%) occurred in the range of 344-440 °C (endo effect 400.3 °C), as a result of which the polyphosphate was transformed into low-temperature metaphosphate B-$Al(PO_3)_3$, stable up to 550-600 °C. The blurred exothermal effect with a maximum of 584.1 °C without changing the substance mass corresponded to the polymorphic transformation of B-$Al(PO_3)_3$ (monoclinic) → A-$Al(PO_3)_3$ (cubic). The high-temperature metaphosphate existed up to 1000-1030 °C, after which it decomposed into aluminum orthophosphate $AlPO_4$ and phosphoric anhydride P_2O_5. The nature of thermograms for binders obtained from gibbsite with different degrees of dehydration remained unchanged. The sequence of transformations obtained does not contradict the literature data.

To explain the differences in the Al compounds dissolution in OPA, a physicochemical analysis of gibbsite and APB samples was performed.

Fig. 4 shows the data of the original gibbsite thermal analysis.

Dehydration occurred in the temperature range of 212-296 °C; the maximum endo effect was at 280 °C. Its presence and mass loss (26.7 %) indicated the hydroxide decomposition to form boehmite: $Al(OH)_3 \rightarrow$ $\rightarrow AlOOH + H_2O$. The estimated value of mass loss according to this equation is 23.1%. This was followed by an extended cleavage of water to form alumina, presumably in the form of γ-Al_2O_3. This process was accompanied by a small endo effect at 494 °C. The total mass loss was 34.7%, which was almost the same as the theoretical value (34.6%).

X-ray phase analysis (Fig. 5) showed that up to 250 °C the main phase was gibbsite, at this temperature boehmite was added to it. Under these conditions, the hydroxide, although mostly retaining its chemical composition, underwent significant structural changes, which contributed to its increased reactivity. Apparently, this is why it actively interacted with OPA, forming an almost homogeneous binder. Boehmite existed up to 450 °C, at which time it began to dehydrate to γ-Al_2O_3.

Based on the fact that the full-width-at-half-maximum (FWHM) of boehmite diffraction peak, and consequently the size of its crystallites, changed by ~17% during the transition from 300 °C to 450 °C, it can be assumed that the intensity of the boehmite reaction with acid also changed.

On the IR spectrum of the gibbsite (Fig. 6), a combination of narrow intense bands was observed at 3629, 3624, 3450, and 3376 cm^{-1}, which fully corresponded to the characteristic valence oscillations of isolated OH-groups of the gibbsite [33]. The deformation oscillations of the H-O-H were corresponded to the band of 1636 cm^{-1}, and the δ(O-H) of the gibbsite – to bands of 1023 and 973 cm^{-1} [33]. This was followed by bands for valence (800-650 cm^{-1}) and deformation (560-525 cm^{-1}) octahedral oscillations of AlO_6

The IR spectra of the gibbsite after heat treatment are shown in Fig. 7. The most significant changes were observed in the high-frequency region: well-resolved bands in the region of 3700-3370 cm^{-1} (Fig. 6) merged into wide bands (Fig. 7) corresponding to the valence oscillations of OH-groups coordinated around Al. Sharp bands of 1023 and 973 cm^{-1}, corresponding to deformation oscillations δ(OH), were smoothed out; their intensity decreased. A band of approx. 490 cm^{-1} appeared; it could be attributed to oscillations in Al^{IV} [34], which intensified with an increase in the heat treatment temperature.

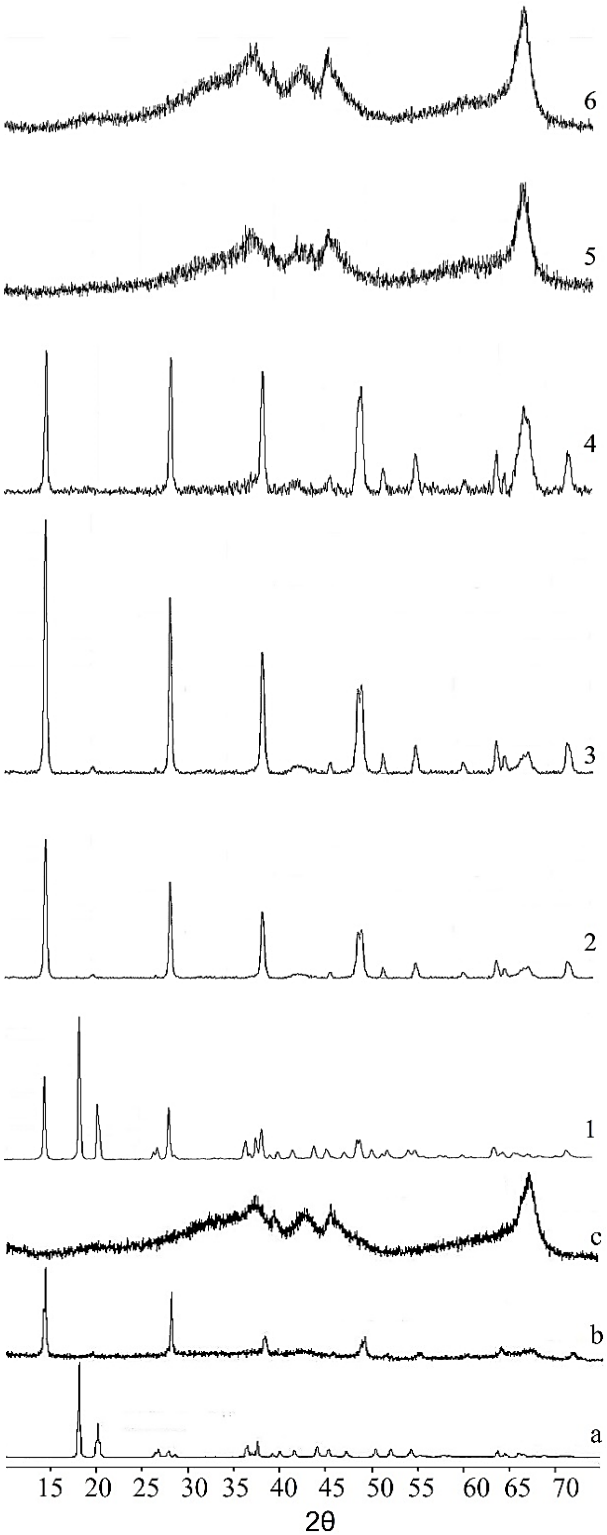

Fig. 5. Diffractograms of gibbsite heat-treated at different temperatures (1-6). Temperature, °C: 1 – 250, 2- 300, 3 – 400, 4 – 450, 5 – 500, 6 – 550. A diagram of standard of gibbsite $Al(OH)_3$ (a), boehmite AlO(OH) (b) and γ-Al_2O_3 (c) are given

Рис. 5. Дифрактограммы гиббсита, термообработанного при различных температурах (1-6). Температура, °C: 1 – 250, 2- 300, 3 – 400, 4 – 450, 5 – 500, 6 – 550. Приведены диаграммы эталонов гиббсита $Al(OH)_3$ (a), бемита AlO(OH) (b) и γ-Al_2O_3 (c)

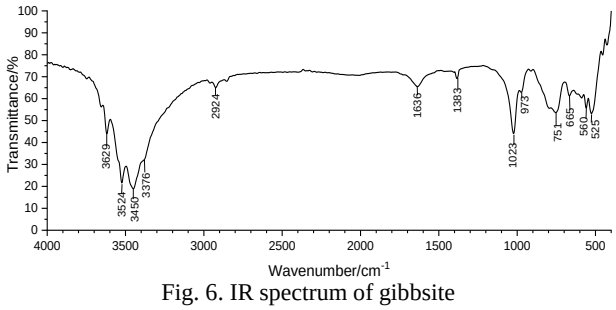

Fig. 6. IR spectrum of gibbsite

Рис. 6. ИК спектр гиббсита

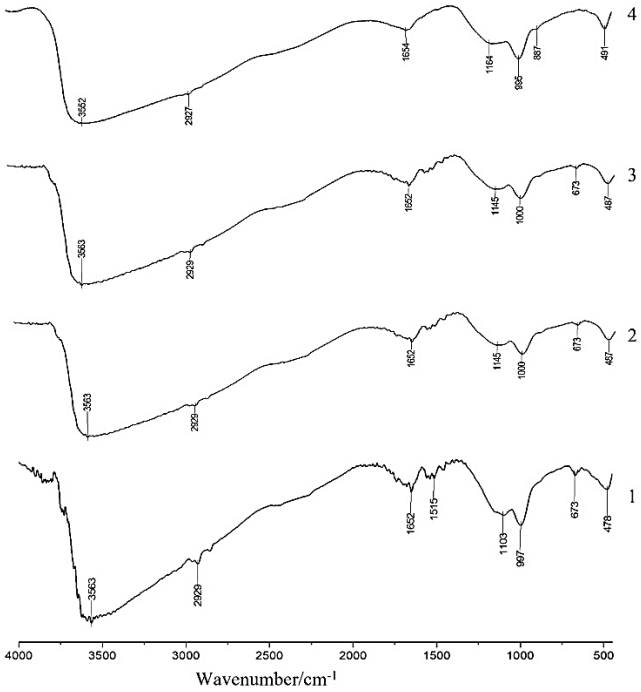

Fig. 7. IR spectra of heat-treated gibbsite. Temperature, °C: 1-200, 2-300, 3-350, 4-400

Рис. 7. ИК спектры гиббсита, подвергнутого термообработке. Температура, °C: 1-200, 2-300, 3-350, 4-400

The IR spectra of the binders obtained by dissolving heat-treated gibbsite in the OPA were taken. For this purpose, the binders were separated by filtration into liquid and solid phases, which were analyzed separately. Examples of spectra are presented in Fig. 8. The analysis of the spectra showed an identical pattern of bands distribution regardless of the gibbsite processing temperature. The IR spectra of the liquid phase contained stretched unresolved bands in the range of 3600-2200 cm^{-1} corresponding to the oscillations of OH groups connected by H-bonds, as well as coordinated around Al^{3+} ions: from asymmetric (3600-3520 cm^{-1}) and symmetrical (3450-3440 cm^{-1}) valence to total deformation and torsional oscillations of water (2300-2100 cm^{-1}), which were confirmed by the presence of deformation oscillations δ(OH) of free (liquid) water (1618-1655 cm^{-1}). In the region of 2800-2300 cm^{-1}, bands from OH groups valence oscillations of acid

phosphates were also superimposed [35]. Wide bands for dried precipitates in the region of high wave numbers did not merge to the same extent as for liquid binders; they also corresponded to oscillations of OH and HOH groups. Bands in the range of 1350-850 cm^{-1} were caused by valence oscillations P-O in hydrated aluminum phosphates [36]. At the same time, in the liquid, the band ~1000 cm^{-1} corresponded to the valence oscillations ν_s(P-OH), while in the solid phase the band was ~1070 cm^{-1} – presumably valence oscillations of P-O-Al bonds [35]. This might indicate the presence of $AlPO_4$ in the sediment. The latter was confirmed to a certain extent by a group of bands 511-503, 634 and 738 cm^{-1}, partially overlapped by bands for oscillations of Al-O bonds. The narrow band of ~490 cm^{-1} could be due to the oscillations of Al^{IV}-O and P-O in the PO_4 group.

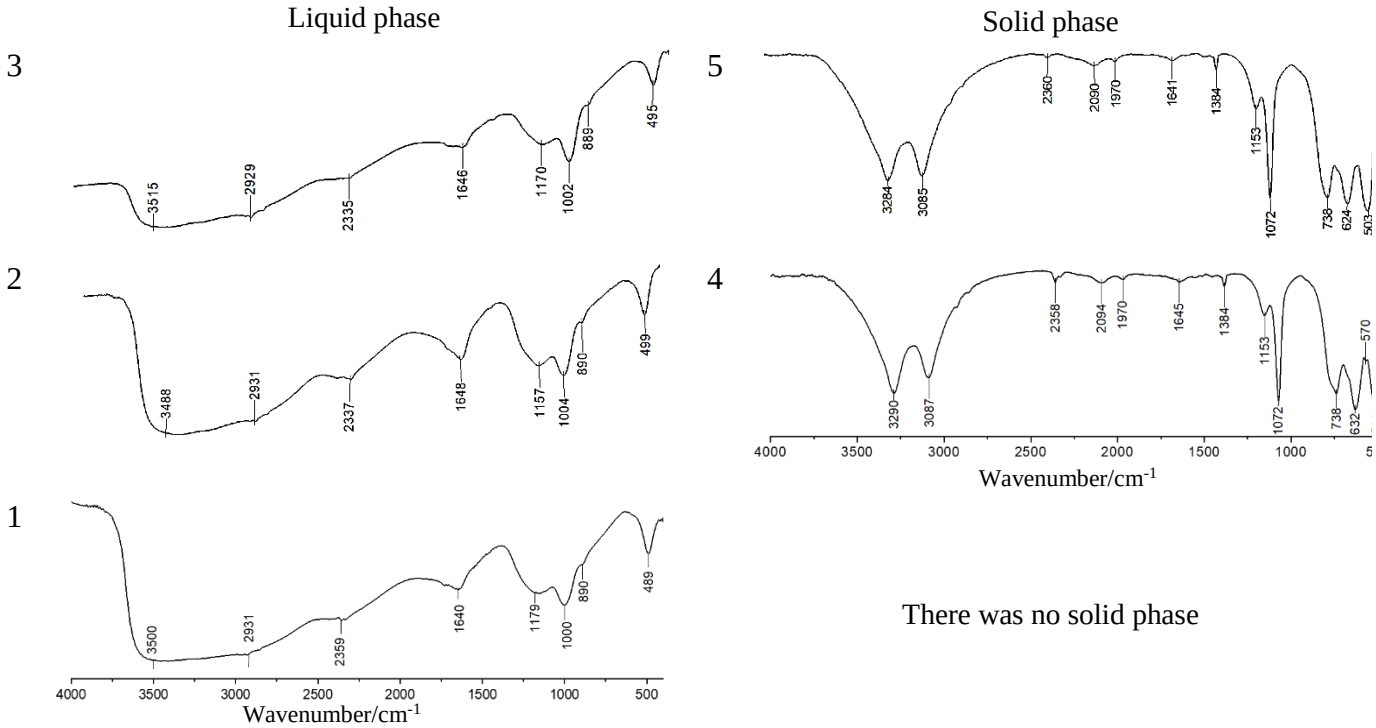

Fig. 8. IR spectra of liquid (1-3) and solid (4-5) fractions of APBs based on gibbsites G200, G300 and G550. Temperature, °C: 1-200; 2, 4 – 300; 3, 5 – 550

Рис. 8. ИК спектры жидкой (1-3) и твердой (4-5) фракций АФС на основе гиббсита Г200, Г300 и Г550. Температура, °С: 1-200; 2, 4 – 300; 3, 5 – 550

The resulting solid phase differed in composition from the liquid one, which meant that filtration was capable of violating the specified P/Al ratio, and the desired characteristics of a binder might not be achieved. Therefore, in the course of synthesis, it is advisable to achieve the most complete dissolution of the substance introducing Al_2O_3, including by increasing the reactivity of the latter. Of the aluminum-containing components studied, the most active can be attributed to bayerite and gibbsite, previously subjected to heat treatment at 200-250 °C.

CONCLUSION

The effect of aluminum-containing component form used for the synthesis of the aluminum-phosphate binder: bayerite and gibbsite, previously heat-treated at 50-550 °C, on the degree of homogeneity of the APB, on which its survivability largely depended, was studied. Using nephelometry, it was established that with a fixed synthesis duration, the minimum degree of turbidity was achieved when gibbsite was dissolved after treatment at 200-250 °C as well as bayerite in orthophosphoric acid. By IR spectra analysis, it was shown that the compositions of the liquid phase and sediment differed regardless of the temperature of the gibbsite heat treatment, which meant that filtration was able to violate the specified P/Al ratio.

ACKNOWLEDGEMENTS

The work was carried out within the framework of the state assignment for the implementation of research work (Topic No. FZZW-2024-0004). The study was carried out using the resources of the Center for Collective Use of Scientific Equipment of ISUCT (with the support of the Ministry of Education and Science of the Russian Federation, agreement No. 075-15-2021-671).

The authors declare the absence a conflict of interest warranting disclosure in this article.

Работа выполнена в рамках государственного задания на выполнение НИР (Тема № FZZW-2024-0004). Исследование выполнено с использованием ресурсов Центра коллективного пользования научной аппаратурой ИГХТУ (при поддержке Минобрнауки России, № 075-15-2021-671).

Авторы заявляют об отсутствии конфликта интересов, требующего раскрытия в данной статье.

REFERENCES
ЛИТЕРАТУРА

1. **Wang M., Liu J., Du H., Hou F., Guo A., Zhao Y., Zhang J.** // *J. Alloy. Compd.* 2014. V. 617. P. 219–221. DOI: 10.1016/j.jallcom.2014.08.043.
2. **Ma C., Chen H., Wang C., Zhang J., Qi H., Zhou L.** // *Materials*. 2017. V. 10. 1266. DOI: 10.3390/ma10111266.
3. **Hahn D., Masoudi Alavi A., Quirmbach P.** // *Mater. Chem. Phys.* 2021. V. 267. 124663. DOI: 10.1016/j.matchemphys.2021.124663.
4. **Wang J., Wu M., Miao X., Wang Y., Bian D., Zhao Y.** // *Colloids Surf. A: Physicochem. Eng. Asp*. 2023. V. 658. 130765. DOI: 10.1016/j.colsurfa.2022.130765.
5. **Luz A.P., Gomes D.T., Pandolfelli V.C.** // *Ceram. Int.* 2015. V. 41. N 7. P. 9041-9050. DOI: 10.1016/j.ceramint.2015.03.276.
6. **Filatova N.V., Kosenko N.F., Maloivan M.S., Zonina I.I.** // *ChemChemTech [Izv. Vyssh. Uchebn. Zaved. Khim. Khim. Tekhnol.]*. 2023. V. 66. N 9. P. 77-82. DOI: 10.6060/ivkkt.20236609.6816. **Филатова Н.В., Косенко Н.Ф., Малоиван М.С., Зонина И.И.** // *Изв. вузов. Химия и хим. технология.* 2023. Т. 66. Вып. 9. С. 77-82. DOI: 10.6060/ivkkt.20236609.6816.
7. **Lopes S.J.S., Luz A.P., Gomes D.T., Pandolfelli V.C.** // *Ceram. Int.* 2017. V. 43. N 8. P. 6239-6249. DOI: 10.1016/j.ceramint.2017.02.023.
8. **Mu Y., Li W., Chen J., Liu H., Wang C., Zhou X., Jiang S., Wang L., He X., Li M., He F.** // *Ceram. Int.* 2024. V. 50. N 11. Part A. P. 18718-18728. DOI: 10.1016/j.ceramint.2024.02.360.
9. **Tricot G., Hu H., Beaussart A., Fernandes I., Perrot C.** // *Materials*. 2022. V. 15. 2337. DOI: 10.3390/ma15062337.
10. **Wang M., Zhang J., Wei T., Zhou Q., Li Z.** // *Int. J. Adhes. Adhes.* 2020. V. 100. 102627. DOI: 10.1016/j.ijadhadh.2020.102627.
11. **Wang Q., Jia D., Duan W., Ma S., Yang H., He P., ZhouY.** // *Colloids Surf. A: Physicochem. Eng. Asp.* 2024. V. 683. 132968. DOI: 10.1016/j.colsurfa.2023.132968.
12. **Cao X., Zhao K., Wang L., Wang T., Wu Y., Tang X., Bai J., Zhang C., Liu L., Cao W., Zhang G.** // *Ceram. Int.* 2024. V. 50. N 13. DOI: 10.1016/j.ceramint.2024.04.097.
13. **Li Y., Chen L., Hong L., Ran K., Zhan Y, Chen Q.** // *J. Alloys Compd*. 2019. V. 785. P. 838–845. DOI: 10.1016/j.jallcom.2019.01.114.
14. **Khamkongkaeo A., Bootchanont A., Klysubun W., Amonpattaratkit P., Boonchuduang T., Tuchinda N., Phetrattanarangsi T., Nuntawong N., Kuimalee S., Lohwongwatana B.** // *Ceram. Int.* 2019. V. 45. P. 1356–1362. DOI: 10.1016/j.ceramint.2018.07.253.
15. **Xu X., Zhang J., Jiang P., Liu D., Jia X., Wang X., Zhou F.** // *Ceram. Int.* 2022. V. 48. P. 864–871. DOI: 10.1016/j.ceramint.2021.09.168.
16. **Jiao C., Hou C., Zhang M., Chao N., Gao Y., Li Y.** // *J. Radioanal. Nucl. Chem.* 2021. V. 329. P. 475–484. DOI: 10.1007/s10967-021-07801-0.
17. **Zulkifly K., Cheng-Yong H., Yun-Ming L., Bayuaji R., Abdullah M.M.A.B., Ahmad S.B., Stachowiak T., Szmidla J., Gondro J., Jez B., Khalid M.S.B., Garus S., Shee-Ween O., Wan-en O., Hui-Teng N.** // *Materials*. 2021. V. 14. 1973. DOI: 10.3390/ma14081973.
18. **Idamayanti D., Nurhakim I.L., Bandanadjaja B., Purwadi W., Lilansa N.** // *IOP Conf. Ser.: Mater. Sci. Eng.* 2019. V. 541. DOI: 10.1088/1757-899X/541/1/012027.
19. **Leng G., Duan S., Liu X., Lin F., Yang Y., Min X., Mi R., Wu X., Liu Y., Fang M., Huang Z.** // *J. En. Storage.* 2022. V. 55. Pt. D. 105815. DOI: 10.1016/j.est.2022.105815.
20. **Jia Y., Wan H., Chen L., Zhou H., Chen J.** // *Surf. Coat. Technol.* 2017. V. 315. P. 490-497. DOI: 10.1016/j.surfcoat.2017.03.013.
21. **Wang M., Li K., Lu R., Feng Z., Wei T., Zhou Q., Zhai W.** // *Ceram. Int.* 2021. V. 47. N 23. P. 32988-33001. DOI: 10.1016/j.ceramint.2021.08.199.
22. **Wu Z., Chen T., Aladejana J.T., Zhang Z., LiangS., Xiao Y., Lin J., Wang X.(A.), Xie Y.** // *RSC Adv.* 2021. V. 11. 34416. DOI: 10.1039/d1ra05552f.
23. **Gou Y., Xie Y., Shen S., Xing H., Jin P., Li H., Chao X., Hu D.** // *Int. J. Adhes. Adhes.* 2024. V. 132. 103685. DOI: 10.1016/j.ijadhadh.2024.103685.
24. **Djobo J.N., Nkwaju R.** // *RSC Adv.* 2021. V. 11. 32258. DOI: 10.1039/d1ra05433c.
25. **Wang Q., Jia D., Duan W., Yang H., Ma S., He P., Colombo P., Zhou Y.** // *J. Alloys Compd*. 2023. V. 966. 171487. DOI: 10.1016/j.jallcom.2023.171487.
26. **Tricot G., Coillot D., Creton E., Montagne L.** // *J. Europ. Ceram. Soc.* 2008. V. 28. N 6. P. 1135-1141. DOI: 10.1016/j.jeurceramsoc.2007.09.046.
27. **Li Y., Chen G., Zhu S., Li H., Ma Z., Liu Y., Liu L.** // *Bull. Mater. Sci.* 2019. V. 42. 200. DOI: 10.1007/s12034-019-1912-3.
28. **Wei H., Wang T., Zhang Q., Jiang Y., Mo C.** // *J. Chin. Chem. Soc.* 2020. V. 67. P. 116–124. DOI: 10.1002/jccs.201900008.
29. **Rousseau G., Montagne L., Méar F.O.** // *J. Europ. Ceram. Soc.* 2021. V. 41. N 9. P. 4970-4976. DOI: 10.1016/j.jeurceramsoc.2021.03.023.
30. **Bemmer V., Bowker M., Carter J.H., Davies P.R., Edwards L.E., Harris K.D.M., Hughes C.E., Robinson F., Morgan D.J., Thomas M.G.** // *RSC Adv.* 2020. V. 10. 8444.
31. **Mocciaro A., Conconi M.S., Rendtorff N.M., Scian A.N.** // *J. Therm. Anal. Calorim.* 2021. V. 144. P. 1083–1093. DOI: 10.1007/s10973-020-10488-2.
32. **Filatova N.V., Kosenko N.F., Artyushin A.S.** // *J. Sib. Fed. Univ. Chem.* 2021. V. 14. N 4. P. 527–538. DOI: 10.17516/1998-2836-0260.
33. **Jiao W.Q., Yue M.B., Wang Y.M., He M.-Y.** // *Micropor. Mesopor. Mater.* 2012. V. 147. N 1. P. 167–177. DOI: 10.1016/j.micromeso.2011.06.012.
34. **Filatova N.V., Kosenko N.F., Denisova O.P., Sadkova K.S.** // *ChemChemTech [Izv. Vyssh. Uchebn. Zaved. Khim. Khim. Tekhnol.]*. 2022. V. 65. N 8. P. 85-93. DOI: 10.6060/ivkkt.20226508.6656. **Филатова Н.В., Косенко Н.Ф., Денисова О.П., Садкова К.С.** // *Изв. вузов. Химия и хим. технология.* 2022. Т. 65. Вып. 8. С. 85-93. DOI: 10.6060/ivkkt.20226508.6656.
35. **Djobo J.N., Stephan D.** // *J. Am. Ceram. Soc.* 2022. N 105. P. 3226–3237. DOI: 10.1111/jace.18333.
36. **Mathivet V., Jouin J., Parlier M., Rossignol S.** // *Mater. Chem. Phys.* 2021. V. 258. 123867. DOI: 10.1016/j.matchemphys.2020.123867.

Поступила в редакцию (Received) 17.05.2024
Принята к опубликованию (Accepted) 30.05.2024